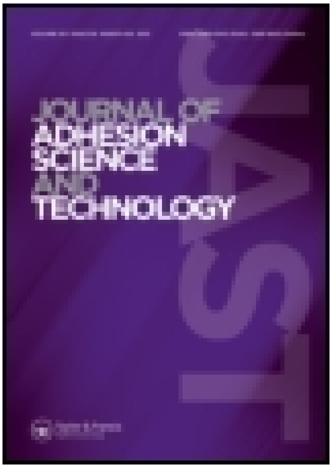

Journal of Adhesion Science and Technology
Publication details, including instructions for authors and subscription information:
http://www.tandfonline.com/loi/tast20

Surface tension parameters of ice obtained from contact angle data and from positive and negative particle adhesion to advancing freezing fronts

C.J. Van Oss [a], R.F. Giese [b], R. Wentzek [c], J. Norris [d] & E.M. Chuvilin [e]

[a] Department of Microbiology, Department of Chemical Engineering

[b] Department of Geology, State University of New York at Buffalo, Buffalo, NY 14241, USA

[c] Department of Geology, State University of New York at Buffalo, Buffalo, NY 14241, USA

[d] Department of Geology, State University of New York at Buffalo, Buffalo, NY 14241, USA

[e] Department of Geology, State University of New York at Buffalo, Buffalo, NY 14241, USA

To cite this article: C.J. Van Oss , R.F. Giese , R. Wentzek , J. Norris & E.M. Chuvilin (1992) Surface tension parameters of ice obtained from contact angle data and from positive and negative particle adhesion to advancing freezing fronts, Journal of Adhesion Science and Technology, 6:4, 503-516, DOI: 10.1163/156856192X00827

To link to this article: http://dx.doi.org/10.1163/156856192X00827

J. Adhesion Sci. Technol. Vol. 6, No. 4, pp. 503–516 (1992)
© VSP 1992.

Surface tension parameters of ice obtained from contact angle data and from positive and negative particle adhesion to advancing freezing fronts

C. J. VAN OSS,[1,2,*] R. F. GIESE,[3] R. WENTZEK,[3] J. NORRIS[3] and
E. M. CHUVILIN[3,†]

Departments of [1] Microbiology, [2] Chemical Engineering and [3] Geology,
State University of New York at Buffalo, Buffalo, NY 14241, USA

Revised version received 13 November 1991

Abstract—From contact angle data obtained on flat ice surfaces with a number of liquids, combined with data on particle and macromolecule adhesion or non-adhesion to advancing freezing fronts, the apolar (Lifshitz–van der Waals or LW) and polar (Lewis acid-base or AB) surface tension (γ) components and parameters have been determined. At 0°C these are $\gamma^{\mathrm{LW}}_{\mathrm{ice}} = 26.9$ and $\gamma^{\mathrm{AB}}_{\mathrm{ice}} = 39.6$ mJ/m^2. The latter consists of an electron-acceptor ($\gamma^{\oplus}$) and an electron-donor ($\gamma^{\ominus}$) parameter: $\gamma^{\oplus} = 14$ and $\gamma^{\ominus} = 28$ mJ/m^2.

Keywords: Surface tension of ice; advancing freezing fronts; particle adhesion; ice fronts; contact angles; surface tension parameters (polar); apolar surface tension component.

1. INTRODUCTION

Earlier work indicated the existence of a direct correlation between attractive (or repulsive) interfacial forces and the engulfment (or the exclusion) of particles suspended in a liquid by a slowly advancing solidification front of the same material as the liquid [1–3]. More recently, an attempt was made to determine the total surface tension of ice, from advancing solidification front interactions between glutaraldehyde-fixed human erythrocytes and advancing ice fronts, in water [4]. The value found was $\gamma^{\mathrm{TOT}}_{\mathrm{ice}} \approx 80.2$ mJ/m^2.[‡] However, in view of the concept then held [4] that γ^{TOT} of any material was indivisible (i.e. any distinction between the apolar and polar components of γ was believed to be

---

[*] To whom correspondence should be addressed.

[†] Permanent address: Department of Geocryology, Moscow State University, 119899, Moscow, USSR.

[‡] As surface tensions, interfacial tensions, and surface free energies have the same dimensions, and can all, under the proper conditions, be added to or subtracted from each other [see, for example, the Dupré equation, quoted below as equation (9)], it has become general practice to express all these entities in the same SI units, using mJ/m^2. All the same, it remains prudent to distinguish clearly between the different functions of these entities. This is done by designating the *surface tension* of a material, *i*, as γ_i; the *interfacial tensions* between two condensed materials, *i* and *j* as γ_{ij}; and free energies of interaction as ΔG. Here ΔG_{ii} indicates the free energy of cohesion of material, *i*; ΔG_{ij} the free energy of adhesion between materials *i* and *j in vacuo*; ΔG_{iji} the free energy of interaction between molecules or particles of material, *i*, immersed in liquid, *j*; and ΔG_{ikj}, the free energy of interaction between molecules or particles of materials *i* and *j* immersed in liquid *k*.

prohibited), and in consideration of the fact that the theoretical basis of that work [4] was founded on an 'equation of state' [5] which has since been shown to be seriously flawed [6–10], no undue weight should be attached to the value of 80.2 mJ/m^2 for the surface tension of ice.

In 1967, Knight [11] reported a (receding) contact angle for water on ice of 12° at a temperature slightly below 0°C. This would imply that the corresponding *advancing* contact angle was somewhat higher (realistically probably of the order of 20°). In 1969, Ketcham and Hobbs [12] reported a contact angle of water on ice, at 0°C, of 20° ± 2°. It thus appears probable that $\gamma_{\text{ice}}^{\text{TOT}}$ is less than $\gamma_{\text{water}}^{\text{TOT}}$ at 0°C; i.e. less than 75.8 mJ/m^2. Adamson *et al.* [13] reported contact angles of CS_2 on polycrystalline ice (at −5°C) of about 20° and on single crystal ice (at 0°C) of about 42°, yielding an apolar or Lifshitz–van der Waals (LW) component of the surface tension of ice, $\gamma_{\text{ice}}^{\text{LW}} \approx 34$ mJ/m^2 for polycrystalline ice at −5°C and $\gamma_{\text{ice}}^{\text{LW}} \approx 26.8$ mJ/m^2 for single crystal ice at 0°C.

With a view to studying the interaction of freezing fronts of ice, in water, with various biological and mineral particles, a study was done to obtain more complete data on the surface tension components and parameters of ice.

2. THEORY

The theory of apolar and acid–base (polar) interfacial interactions has been extensively treated elsewhere [7–14]; therefore, only the essentials are given here. The total surface tension of a given (non-metallic) material (i) is the sum of its apolar and polar components:

$$\gamma_i = \gamma_i^{\text{LW}} + \gamma_i^{\text{AB}}, \tag{1}$$

where LW indicates the total apolar, Lifshitz–van der Waals interaction, and AB the (Lewis) acid–base, or electron-acceptor/electron-donor, interaction.

The total acid–base free energy of interaction between two polar materials i and j involves two independent interactions and hence must be expressed as [7]:

$$\Delta G_{ij}^{\text{AB}} \equiv -2(\sqrt{\gamma_i^{\oplus}\gamma_j^{\ominus}} + \sqrt{\gamma_i^{\ominus}\gamma_j^{\oplus}}), \tag{2}$$

where $\gamma^{\oplus}$ is the electron-acceptor parameter and $\gamma^{\ominus}$ the electron-donor parameter of the surface tension. As we may state that

$$\Delta G_{ii}^{\text{AB}} = -2\gamma_i^{\text{AB}}, \tag{3}$$

it follows from equations (2) and (3) that

$$\gamma_i^{\text{AB}} = 2\sqrt{\gamma_i^{\oplus}\gamma_i^{\ominus}}. \tag{4}$$

Using the Young–Dupré equation in the form of

$$(1 + \cos\theta)\gamma_i = -\Delta G_{ij} \tag{5}$$

(where i denotes the liquid with which contact angles were determined on a solid, j), the total interfacial (IF) free energy may be expressed [cf. equations (1) and (3)] as

$$\Delta G_{ii}^{\text{IF}} = \Delta G_{ii}^{\text{LW}} + \Delta G_{ii}^{\text{AB}} \tag{6a}$$

and as

$$\Delta G_{ij}^{\mathrm{IF}} = \Delta G_{ij}^{\mathrm{LW}} + \Delta G_{ij}^{\mathrm{AB}}. \tag{6b}$$

We may then, by combining equations (1), (2), (4), and (6b), express the Young–Dupré equation (5) as

$$(1 + \cos\theta)\gamma_i = 2(\sqrt{\gamma_i^{\mathrm{LW}}\gamma_j^{\mathrm{LW}}} + \sqrt{\gamma_i^{\oplus}\gamma_j^{\ominus}} + \sqrt{\gamma_i^{\ominus}\gamma_j^{\oplus}}). \tag{7}$$

In this equation it should be noted that

$$\gamma_{ij}^{\mathrm{LW}} = (\sqrt{\gamma_i^{\mathrm{LW}}} - \sqrt{\gamma_j^{\mathrm{LW}}})^2 \tag{8}$$

and according to the Dupré equation, for interaction in air or *in vacuo*

$$\Delta G_{ij}^{\mathrm{LW}} = \gamma_{ij}^{\mathrm{LW}} - \gamma_i^{\mathrm{LW}} - \gamma_j^{\mathrm{LW}}, \tag{9}$$

so that

$$\Delta G_{ij}^{\mathrm{LW}} = -2\sqrt{\gamma_i^{\mathrm{LW}}\gamma_j^{\mathrm{LW}}}. \tag{10}$$

In all the above expressions of the Young equation, *i* stands for liquid and *j* for solid, but in equations (1)–(4), (6a), (6b), and (8)–14) (see also below), *i* and *j* may be any condensed-phase material.

The values for γ_j^{LW}, $\gamma_j^{\oplus}$, and $\gamma_j^{\ominus}$ can be determined by contact angle (θ) measurements using equation (7). Clearly, to solve for γ_j^{LW}, $\gamma_j^{\oplus}$, and $\gamma_j^{\ominus}$, contact angle measurements must be done with three different, completely characterized liquids (i), of which two must be polar.

Once γ_i^{LW}, $\gamma_i^{\oplus}$, and $\gamma_i^{\ominus}$, as well as γ_j^{LW}, $\gamma_j^{\oplus}$, and $\gamma_j^{\ominus}$, are determined for two different materials *i* and *j*, their interfacial tension γ_{ij} follows from the Dupré equation (9) and equations (1), (2), and (4):

$$\gamma_{ij} = (\sqrt{\gamma_i^{\mathrm{LW}}} - \sqrt{\gamma_j^{\mathrm{LW}}})^2 + 2\sqrt{\gamma_i^{\oplus}\gamma_i^{\ominus}} + \sqrt{\gamma_j^{\oplus}\gamma_j^{\ominus}} - \sqrt{\gamma_i^{\oplus}\gamma_j^{\ominus}} - \sqrt{\gamma_i^{\ominus}\gamma_j^{\oplus}}). \tag{11}$$

From equations (2), (3), (6b), and (10) various free energies of interaction can be obtained:

$$\Delta G_{iji}^{\mathrm{IF}} = -2\gamma_{ij}. \tag{12}$$

According to the Dupré equation for interactions between particles or molecules *i* and *j* in a liquid *k*:

$$\Delta G_{ikj}^{\mathrm{IF}} = \gamma_{ij} - \gamma_{ik} - \gamma_{jk}. \tag{13}$$

The interaction between particles or molecules *i* and *j* immersed in a liquid *k* can then be expressed, using equations (11) and (13), as:

$$\begin{aligned}\Delta G_{ikj}^{\mathrm{IF}} = \gamma_{ij}^{\mathrm{LW}} - \gamma_{ik}^{\mathrm{LW}} - \gamma_{jk}^{\mathrm{LW}} + 2[&\sqrt{\gamma_k^{\oplus}}(\sqrt{\gamma_i^{\ominus}} + \sqrt{\gamma_j^{\ominus}} - \sqrt{\gamma_k^{\ominus}}) \\ &+ \sqrt{\gamma_k^{\ominus}}(\sqrt{\gamma_i^{\oplus}} + \sqrt{\gamma_j^{\oplus}} - \sqrt{\gamma_k^{\oplus}}) - \sqrt{\gamma_i^{\oplus}\gamma_j^{\ominus}} - \sqrt{\gamma_i^{\ominus}\gamma_j^{\oplus}}].\end{aligned} \tag{14}$$

If, in addition, an electrostatic interaction occurs, one can obtain the total free energy of interaction by adding the electrostatic (EL) energy term:

$$\Delta G^{\mathrm{TOT}} = \Delta G^{\mathrm{IF}} + \Delta G^{\mathrm{EL}}, \tag{15}$$

where ΔG^{EL} may be derived from the surface, or ψ_0 potential, of the material in question immersed in a given liquid medium [7].

3. MATERIALS AND METHODS

3.1. Ice

The samples of ice were prepared by slow freezing of deionized (and activated charcoal-adsorbed) water (resistivity $>2\times10^6\ \Omega$ cm) contained in a polyethylene cup. Once frozen, the ice sample was removed and stored in a thermostated box along with the test liquids for the contact angle measurements. Just prior to making contact angle measurements, a smooth, flat surface on the ice sample was formed by careful scraping with a clean microtome knife.

3.2. Clay

The clay mineral used in the freezing front experiments was a standard montmorillonite (a swelling clay mineral from Wyoming) obtained from the Clay Minerals Repository of the Clay Minerals Society (designated SWy-1). Samples of the smectite clay SWy-1 were size-fractionated to exclude all particles greater than 2 μm (e.s.d.). No further treatments were performed on this material. Swelling clay minerals, such as SWy-1, have hydrophilic surfaces. These materials can be modified to become hydrophobic by covering the particle surfaces with a suitable organic material. This is conveniently done by ion-exchanging the surface cations of SWy-1 (largely sodium) with a quaternary ammonium salt [14]. For the present experiments, the salt was hexadecyltrimethyl ammonium bromide (HDTMA) (Fisher Reagent Grade). The exchange was effected by dispersing a sample of SWy-1 in distilled water and adding an aqueous solution of HDTMA (0.1 M) sufficient to satisfy the cation exchange capacity of the clay mineral. Subsequently, the SWy-1:HDTMA was washed with distilled water and finally with ethanol to remove any excess HDTMA. The treated clay was recovered by centrifugation and subsequent drying in an oven at 105°C.

3.3. Freezing front experiments

As water freezes, suspended particulate matter encounters a moving boundary separating the expanding ice from the surrounding water. Whether the particles are excluded or not from the ice is determined by a number of factors: the rate of advance of the ice front; the values of the surface tension components of ice, water, and the suspended particles; and any electrostatic interaction between the particles and the ice front. Swelling clay minerals are very variable materials due largely to different degrees of ionic substitution, different types of substituting ions, and the sites of this substitution (i.e. tetrahedral or octahedral). These differences are reflected in the values of the surface tension components. Thus, in theory, one can select a specific clay mineral whose measured surface tension components are greater or smaller than those of water. These materials are not completely homogeneous, so that individual particles of a smectite clay sample will have values of the surface tension components which are slightly larger or slightly smaller than the measured (weighted average) values. Such a sample would be partly engulfed and partly excluded by the advancing ice front. This phenomenon was used in the present study to obtain an estimate of the values of the AB parameters.

The freezing experiments were performed by placing one end of a closed transparent plastic cylinder (7.2 mm diameter, 130 mm long) so that it was vertically oriented and in contact with a refrigerated cold surface kept at approximately −40°C. The cold surface and plastic cylinder were encased by approximately 50 mm of foam plastic insulation and the uninsulated top end of the plastic cylinder was in contact with a water-filled container acting as a high thermal mass. The cylinder was filled with a clay–water suspension of 0.5–2.0% (w/w) solids content. Freezing began at the cold surface and progressed vertically along the axis of the cylinder. As the freezing front moved away from the interface with the cold surface, the velocity of advance of the ice gradually decreased. An actual experiment used two identical cylinders, one for the engulfment/exclusion experiment and the second for the measurement of the rate at which the freezing front advanced. The rate of advance was determined by measuring the position of the ice front by means of a measuring rod which was lowered into the cylinder until it encountered the ice front. These measurements were done on an hourly basis to generate a curve of ice position in the cylinder vs. time.

After the termination of a freezing experiment, the test cylinder was removed and examined visually to determine the extent of engulfment and/or exclusion of the clay particles by the ice. The top 5 mm or so remained unfrozen in a typical experiment, so that any excluded clay collected at the bottom of the water column in contact with the ice. Subsequent examination of the frozen sample involved removing the ice from the plastic cylinder, splitting it longitudinally, and examining a smoothed surface with a microscope. In practice, the initial high rate of freezing (approximately 3 mm/h) engulfed not only clay particles, but also air bubbles. The very slowest freezing rates (<0.5 mm/h) at the top of the ice column were used to determine whether the clay particles were excluded by the freezing front. Thus, a short section of clear ice at the top of the frozen column with an accumulation of clay lying at the ice–water interface was taken as evidence that exclusion had occurred.

3.4. Contact angle measurements

The measurements of contact angles of test liquids on ice were done in the Ice Core Laboratory of the Geology Department at SUNY Buffalo, where the ambient temperature is −20°C. The desired temperature for most measurements was higher than −20°C, so an insulated enclosure was built from foam plastic insulation. The internal temperature was regulated by a heating tape and Variac. All the test liquids and the ice samples were stored in this enclosure. A telemicroscope (Gaertner model M101AT) was placed outside the container such that the top surface of an ice specimen inside the enclosure could be viewed through a small hole in the end of the container. A hole in the top of the insulated container allowed a long Pasteur pipet (Fisher Scientific, 13-678-7C) to place drops of a test liquid on the ice surface. The contact angle measurements were made with a goniometer eyepiece, provided with cross-hairs and mounted on the telemicroscope. A drop of a test liquid was placed on the ice surface inside the heated enclosure and, if possible, both sides of the drop were measured. Contact angles are normally measurable with a precision of ±2°, but when a number of measurements are made, the precision extends to at least the first decimal, depending on the number of measurements.

The liquids used for contact angle measurements were *cis*-decahydronaphthalene (*cis*-decalin) and aqueous solutions of 55% sucrose and 34% $MgCl_2$ (w/w); these liquids and the liquids used for contact angle measurements on polymethylmethacrylate all comprise analytical-grade quality compounds or better. Especially diiodomethane is always used as fresh as possible and conserved in complete darkness. It should be noted that diiodomethane, α-bromonaphthalene, water, and formamide cannot be used at sub-freezing temperatures, while glycerol and ethylene glycol spread on ice.

4. RESULTS

4.1. Contact angles

Finite contact angles were obtained with *cis*-decalin (*cis*-decahydronaphthalene) and with solutions of 55% (w/w) sucrose in water and of 34% (w/w) $MgCl_2$ in water (see Table 1).

Table 1.
Average contact angles of liquids on ice at various temperatures

Liquid	Average contact angle (°)	Temperature (°C)
Decalin[a]	30.3	−6
	26.3	−10
	15.0	−20
55% Sucrose	12.3	−8
34% $MgCl_2$	10.3	−20

[a] $\gamma^{LW} = 32.2$ mJ/m² [15].

4.2. Lifshitz–van der Waals surface tension component of ice from the decalin contact angles

The surface tensions of *cis*-decalin (γ_L) at different temperatures are given by Jasper [15] as follows: at −20°C, $\gamma_L = 36.8$; at −10°C, $\gamma_L = 36.65$; and at 0°C, $\gamma_L = 34.5$; so that (by interpolation) at −8°C, $\gamma_L = 35.4$ mJ/m². For all practical purposes, decalin may be taken to be apolar, so that, for decalin, $\gamma_L = \gamma_L^{LW}$. From the above values [using equation (7)] and from the contact angles given in Table 1, by least-squares analysis, $\gamma^{LW} \approx 29.6$ mJ/m² at 0°C.

4.3. Surface tension parameters of 55% sucrose and 34% $MgCl_2$ solutions by contact angle determination on PMMA

Contact angles of the 55% aqueous solution (w/w) of sucrose and of the 34% aqueous solution (w/w) of $MgCl_2$ were determined on freshly cast layers of polymethylmethacrylate (PMMA) (deposited on glass slides from a 6% solution of PMMA in toluene, evaporated in air, and kept in a vacuum desiccator, over Drierite), see Table 2. The surface tension components and parameters of the liquids used, as well as of 55% sucrose and 34% $MgCl_2$ deduced from these contact angle measurements on PMMA, are given in Table 3.

Table 2.
Contact angles of liquids on PMMA at 20°C

Liquid	Average contact angle (°)
Diiodomethane	32.0
α-Bromonaphthalene	69.0
Water	59.3
Glycerol	62.3
Formamide	50.0
Ethylene glycol	44.8
55% (w/w) sucrose in water	58.8
34% (w/w) $MgCl_2$ in water	75.5

Table 3.
Surface tension components and parameters of liquids (at 20°C, in mJ/m^2) used for contact angle determinations on PMMA, and of PMMA, 55% sucrose, and 34% $MgCl_2$ derived from these contact angle determinations

Liquid	γ^{TOT}	γ^{LW}	γ^{AB}	$\gamma^{\oplus}$	$\gamma^{\ominus}$
Diiodomethane[a]	50.8	50.8	0	0	0
α-Bromonaphthalene[a]	44.4	44.4	0	0	0
Water[a]	72.8	21.8	51.0	25.5	25.5
Glycerol[a]	64.0	34.0	30.0	3.92	57.4
Formamide	58.0	39.0	19.0	2.28	39.6
Ethylene glycol[b]	48.0	29.0	19.0	1.92	47.0
55% Sucrose (w/w in water)	75.7[c]	28.8[d]	46.9	24.63[e]	22.32[e]
34% $MgCl_2$ (w/w in water)	93.5[c]	25.6[f]	67.9	31.61[e]	36.47[e]
PMMA (solid)	42.7	42.7	0	0	20.4

[a] See van Oss *et al.* [16].

[b] γ_L^{TOT}, γ_L^{LW}, and γ_L^{AB} data from Chaudhury [26]; the $\gamma_L^{\oplus}$ and $\gamma_L^{\ominus}$ parameters were obtained from known γ_L^{AB} values and from the solubility of ethylene glycol (EG) in water (3.168 mol/l) and an estimated contractable surface area between two EG molecules of about 0.2 nm^2 (van Oss, unpublished results).

[c] From surface tension data: *CRC Handbook of Chemistry and Physics* (51st edn, 1970/71).

[d] From $\gamma^{\oplus} = 42$ mJ/m^2 for solid sucrose (van Oss, in preparation) and the volume ratio of sucrose in 55% (w/w) aqueous solution [= 34.8% (v/v), given a density of sucrose of 1.58].

[e] From the contact angle data given in Table 2 and the value of γ_L^{AB} $(= 2\sqrt{\gamma_L^{\oplus}\gamma_L^{\ominus}})$.

[f] By analogy with other salts of known γ^{LW}, it can be estimated that γ^{LW} for the $MgCl_2$ solution lies between 45 and 50 mJ/m^2. A value of $\gamma^{LW} = 47.5$ was thus adoped. The concentration (34% $MgCl_2$, w/w) and the density of $MgCl_2$ of 2.316 yield a (v/v) concentration of 14.7%.

4.4. Polar surface tension parameters of ice

From the γ_{ice}^{LW} value (obtained with *cis*-decalin) and the contact angles obtained on ice with 55% sucrose at −8°C and with 34% $MgCl_2$ at −20°C, one obtains an average value for ice of $\sqrt{\gamma^{\oplus}\gamma^{\ominus}} = 24.0$ mJ/m^2 at −8°C and $\sqrt{\gamma^{\oplus}\gamma^{\ominus}} = 30.2$ mJ/m^2 at −20°C, using the data given in Tables 1 and 3. Extrapolation to 0°C then yields $\sqrt{\gamma_{ice}^{\oplus}\gamma_{ice}^{\ominus}} \approx 19.8$ mJ/m^2 for ice. (It should be realized that with 55% sucrose a temperature no lower than ≈ −8°C can be used before freezing of the drop sets in. On the other hand, with 34% $MgCl_2$ the lowest possible temperature had to be used, which in our case was −20°C, to obviate melting the ice by interaction with the salt. Thus, for extrapolation to 0°C, contact angles obtained with two different liquids had to be used.) The data given above do not allow the precise determination of the individual values of $\gamma_{\text{ice}}^{\oplus}$ and $\gamma_{\text{ice}}^{\ominus}$. However, by also taking into account some of the other known properties of ice at 0°C, such as the exclusion of biopolymers (proteins or polysaccharides) and of certain clay particles by advancing freezing fronts of ice, the most plausible value for $\gamma_{\text{ice}}^{\oplus}/\gamma_{\text{ice}}^{\ominus}$ can be deduced in conjunction with the known value for $\sqrt{\gamma_{\text{ice}}^{\oplus}\gamma_{\text{ice}}^{\ominus}} \approx 19.8$ mJ/m².

Extrapolation of the surface tension components and parameters for water at 0°C yields $\gamma_{\text{W}}^{\text{TOT}} = 75.8$, $\gamma_{\text{W}}^{\text{LW}} = 22.8$, $\gamma_{\text{W}}^{\text{AB}} = 53.0$, and $\gamma_{\text{W}}^{\oplus} = \gamma_{\text{W}}^{\ominus} = 26.5$ mJ/m² (assuming that the $\gamma_{\text{W}}^{\oplus}/\gamma_{\text{W}}^{\ominus}$ ratio remains unaltered upon cooling to 0°C). Taking a typical carbohydrate biopolymer, such as dextran [17] or ficoll, or hydrated plasma proteins [18, 19], one may take their surface tension characteristics to be typically $\gamma^{\text{LW}} = 42.0$, $\gamma^{\oplus} = 0$, and $\gamma^{\ominus} = 55$ mJ/m². Using the free energy of interaction between two materials (i and j) dissolved or immersed in a liquid (k) such as water at 0°C, it is possible to express the sign and value of ΔG_{ikj} [see equation (14)].

Now it is known that polysaccharides (ficoll), as well as serum albumin [20] and serum globulins [21] in aqueous solution all are initially repelled by an advancing freezing front. Thus, the value of ΔG_{ikj} (where i is a typical biopolymer, j is ice and k is water at 0°C) for such a system must be positive. If one calculates the values of ΔG_{ikj} with $R = \gamma_{\text{ice}}^{\oplus}/\gamma_{\text{ice}}^{\ominus}$ ratios of 13/30.15, 14/28, 15/26.13, 16/24.5, and 17/23.07 (see Table 4), then it becomes clear that for ΔG_{ikj}, for typical biopolymers, to be positive, the ratio R must be equal to or smaller than 17/23.07, and probably significantly smaller than that, to attain a sufficiently large positive value of ΔG_{ikj}.

Table 4.
Values of ΔG_{ikj}, the free energy of interaction between a typical biopolymer (i) and ice (j) at 0°C, immersed in water or glycerol (k), in mJ/m², for various ratios $R = \gamma_{\text{ice}}^{\oplus}/\gamma_{\text{ice}}^{\ominus}$

	$R = 13/30.15$	14/28	15/26.13	16/24.5	17/23.06
Biopolymer and ice in water:	$\Delta G_{ikj} = +8.3$	+5.6	+3.1	+0.9	−1.2
Biopolymer and ice in glycerol:	$\Delta G_{ikj} = -7.4$	−8.1	−8.8	−9.4	−9.9

In glycerol, typical biopolymers of the kind described above are not repelled but become included by an advancing freezing front, which is one of the principal reasons for the cryoprotective properties of cells of relatively low self-hydrogen-bonding water-miscible organic solvents like glycerol. (It should be noted that it is largely due to the presence of outer coating, or glycocalyx, of cells, which mainly consists of biopolymer strands of the same properties as the biopolymers described above [22, 23], that the cryoprotectant properties of glycerol apply to cells.) Table 4 also shows that in glycerol the values of ΔG_{ikj} for such biopolymers are negative for all ratios R studied.

To pinpoint the ratio $R = \gamma_{\text{ice}}^{\oplus}/\gamma_{\text{ice}}^{\ominus}$ more closely, freezing experiments were done with suspensions of montmorillonite (SWy-1) clay particles. In Table 5

Table 5.
Values of ΔG_{ikj}, the free energy of interaction between the montmorillonite clay, SWy-1:HDTMA (i), and ice (j) at 0°C, immersed in water (k), in mJ/m^2, for various ratios $R = \gamma^{\oplus}_{\text{ice}}/\gamma^{\ominus}_{\text{ice}}$

	R = 13/30.15	14/28	15/26.13	16/24.5	17/23.06
SWy-1 and ice in water:	$\Delta G_{ikj} = +2.3$	+0.1	−1.8	−3.5	−5.1
SWy-1:HDTMA and ice in water:	$\Delta G_{ikj} = -4.0$	−5.4	−6.7	−7.8	−8.7

ΔG_{ikj} values are given for SWy-1, as well as for SWy-1 treated with hexadecyltrimethylammonium salt (HDTMA), under conditions of the same array of R values, i.e. R = 13/30.15, 14/28, 15/26.13, 16/24.5, and 17/23.06. Values for the surface tension components and parameters of similar clays have been given earlier [24]. Here very slightly different values were used (J. Norris, in preparation) for SWy-1 and SWy-1:HDTMA. For the SWy-1 samples used in these experiments, see Table 6. In Fig. 1 the results of freezing experiments with SWy-1 and SWy-1:HDTMA are shown: SWy-1:HDTMA is completely engulfed by the advancing ice-front, while SWy-1 is partly engulfed and partly rejected by the advancing ice-front. We were fortunate to identify a clay sample of which about half of the particles were engulfed by an advancing freezing front (of ice), for a length of about three-quarters of the freezing path, while the other half of the particles continued to be expelled by the advancing front (Fig. 1B). It may thus be concluded that, on average, the free energy of interaction of SWy-1 with ice in water at 0°C is very close to zero. The value of $R = \gamma^{\oplus}_{\text{ice}}/\gamma^{\ominus}_{\text{ice}}$ which fits these observations best is R = 14/28, with a ΔG_{ikj} value of +0.1 (see Table 5). The inclusion of SWy-1:HDTMA, on the other hand, is compatible with all the R values shown (Fig. 1A).

The best values for the surface tension of ice that can be ascertained to date are summarized in Table 7.

Table 6.
Values of the surface tension components and parameters of the montmorillonite clays SWy-1 and HDTMA-treated SWy-1 used in the freezing experiments (from J. Norris, in preparation), in mJ/m^2

	γ^{LW}	$\gamma^{\oplus}$	$\gamma^{\ominus}$
SWy-1	42.0	0.008	30.2
SWy-1:HDTMA	41.0	0.25	12.4

Table 7.
Surface tension components and parameters of ice and water at 0°C, in mJ/m^2

	γ	γ^{LW}	γ^{AB}	$\gamma^{\oplus}$	$\gamma^{\ominus}$
Ice	69.2	29.6	39.6	14	28
Water	75.8	22.8	53	26.5	26.5

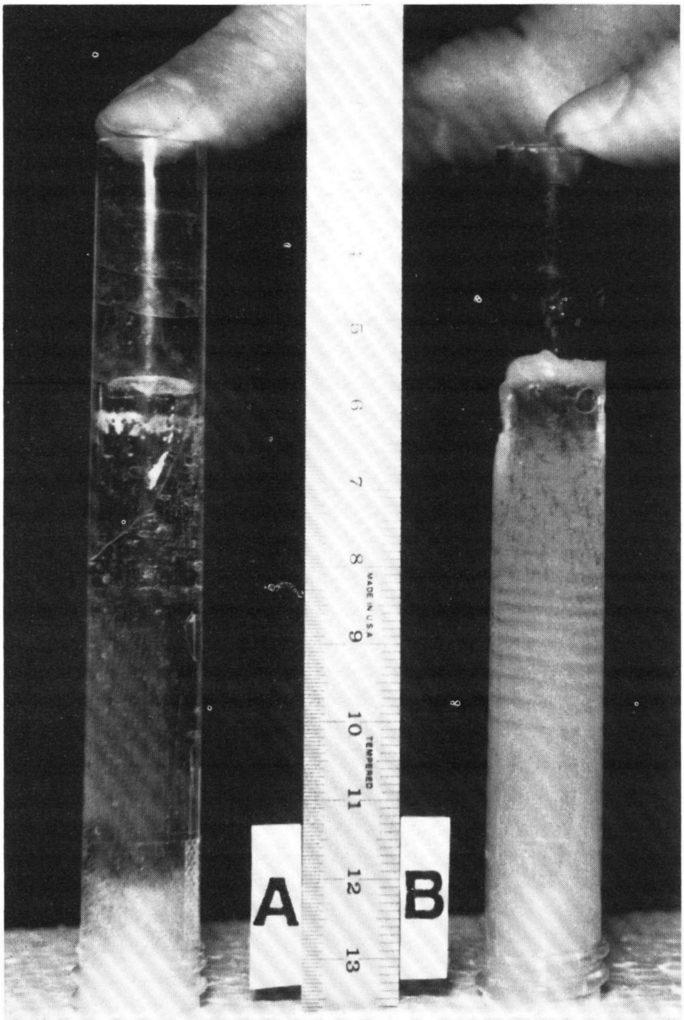

Figure 1. Freezing of (A) SWy-1:HDTMA (montmorillonite clay particles made 'hydrophobic' by treatment with HDTMA, see text) and (B) SWy-1 (the original hydrophilic montmorillonite clay particles). The 'hydrophobic' SWy-1:HDTMA particles are completely engulfed by the advancing ice-front (A), whilst the hydrophilic SWy-1 particles are partly engulfed and partly rejected by the advancing ice-front (see especially the top of tube B).

5. DISCUSSION

5.1. The apolar (LW) surface tension component of ice

The value of $\gamma^{LW} = 29.6$ mJ/m^2 found for ice at 0°C by means of contact angle measurements with *cis*-decalin agrees satisfactorily with the values obtained from the CS$_2$ contact angle data reported by Adamson *et al.* [13], yielding $\gamma^{LW} = 26.8$ mJ/m^2 for monocrystalline ice at 0°C and $\gamma^{LW} = 34.0$ mJ/m^2 for polycrystalline ice (at -5°C) (see also ref. [25]). The ice that we used should be considered polycrystalline; however, it is not immediately obvious why there would be a marked difference between the apolar properties of polycrystalline and single crystal ice. With quartz as well as with calcite crystals we found no significant differences in the γ^{LW} values measured on different crystal faces (Giese, Murphy and van Oss, in preparation). If there is no compelling difference between the γ^{LW} values of different ice faces, then our value of $\gamma_{ice}^{LW} = 29.6$ mJ/m^2 is very close to the average of the two values obtained from the data given by Adamson *et al.* [13]. On the other hand, there may have been a difference in smoothness or contamination: according to Adamson *et al.* [13], the monocrystalline ice faces (but not, apparently, the polycrystalline ones) were polished with lens paper before use. Smoother surfaces give rise to somewhat lower contact angles (see, for example, ref. [26]) which result in somewhat higher γ values. Our ice surfaces were shaved just before use (to be sure that uncontaminated surfaces were obtained) but not polished, as polishing involves the possibility of enhancing surface contamination, and surface contamination, as well as increased smoothness, can lead to changes in γ^{LW}.

The fact that γ_{ice}^{LW} is about 30% higher than γ_{water}^{LW} (at 0°C $\gamma_{water}^{LW} \approx 22.8$ mJ/m^2, see above) appears plausible, considering the more prominent exposure of oxygen atoms at the surface of ice, which follows from the lower $\gamma^{\oplus}/\gamma^{\ominus}$ value of ice compared with water.

5.2. *The polar (AB) surface tension parameters of ice*

From the data shown in Table 4 on the rejection of neutral biopolymers by advancing freezing fronts, it is clear that the value of $R = \gamma_{ice}^{\oplus}/\gamma_{ice}^{\ominus}$ has to be smaller than 17/23.07.

From the data shown in Table 5 on the partial rejection and partial engulfment of particles of the montmorillonite clay SWy-1 by an advancing front, it may be deduced that the value of R for ice is very close to 14/28. The only incertitude here lies in the unknown factor of the electrical surface (ζ) potential of ice in distilled water. The ζ potential of SWy-1 is approximately -45 mV (J. Norris, in preparation). In the absence of dissolved ions, it is not likely that the ζ potential of ice is more negative than ≈ 20 mV. Equating these ζ potentials, for the moment, with their ψ_0 potential (a plausible approximation in view of the extremely low ionic strength of the liquid medium), the aggregate ψ_0 potential (equal to $\sqrt{\psi_{01}\psi_{02}}$) then should not have been more than 30 mV, and quite likely considerably less. For irregularly shaped particles (SWy-1) interacting with a flat ice front, attraction at $\psi_0 = 30$ mV is still possible at $R = 16/24.5$, but not at $R = 14/28$.

LeFebre [27] discussed the possible occurrence, and Gross [28] treated the theoretical aspects of freezing potentials (of ≈ 1–16 V) existing between advancing ice fronts and the water phase, in the presence of fairly low concentrations (10^{-3}–10^{-5} M) of salts such as KF or NH_4Cl, or acids such as HF or HCl. These freezing potentials appeared to be highest at the fastest advancing front velocities and tended to disappear at ionic strengths higher than 10^{-4}–10^{-3} M [27]. It is unclear whether this freezing potential plays a role in the repulsion of solutes or particles by the advancing front. On the whole, it appears unlikely for several reasons:

(a) Freezing ice fronts repel totally uncharged solutes (polysaccharides, gamma-globulins) as readily as charged solutes or particles [20, 21].

(b) If freezing potentials played a role, the repulsion would be enhanced at higher front velocities [27]; however, the opposite occurs [1].

The change of repulsion to attraction which occurs upon the admixture of glycerol to, for example, freezing media for living cells (to obviate cell lysis through the compaction of the cells into too small a volume) correlates well with the results given in Table 4. According to these results, an *attraction* should occur in glycerol between ice and the biopolymers which are typical for the glycocalyx of, for example, erythrocytes (see ref. [22]). Here also electrostatic effects play no major role; for example, the decrease in dielectric constant of, for instance, 33% glycerol in water is only about 15.5%, and the cryoprotective effect of glycerol also holds for cells with considerably lower ζ potentials than erythrocytes (about 18 mV) [29].

5.3. *The total surface tension of ice*

Whilst the total surface tension of a liquid (γ_L) is an important concept, as it plays a crucial role in Young's equation [equation (7)], the total surface tension of a solid (γ_S) plays no role whatsoever in any of the crucial equations [equations (2)–(7) and (11)–(14)] that yield the various free energies of interactions, see, for example, ref. [8]. Nevertheless, it is perfectly permissible to express γ_S, as it signifies, after all, minus one-half of the free energy of cohesion:

$$\Delta G_{ii}^{\mathrm{coh}} = -2\gamma_i. \tag{16}$$

As was already predicted, on general grounds, from the fact that water has a finite contact angle when deposited on ice ($\theta \approx 20°$), $\gamma_{\mathrm{ice}} < \gamma_{\mathrm{water}}$: i.e. $\gamma_{\mathrm{ice}} = 69.2$ mJ/m^2 [cf. equations (1) and (4)], whereas $\gamma_{\mathrm{water}} = 75.8$ mJ/m^2 at 0°C (see Table 7). However, it should be kept in mind that for solids it is only γ_S^{LW}, $\gamma_S^{\oplus}$, and $\gamma_S^{\ominus}$ that count.

5.4. *The contact angle of ice on water*

Using equation (7), it follows that according to our best data for ice at 0°C (Table 7), $\theta_{\mathrm{water\ on\ ice}} = 24.2°$. This is reasonably close to the contact angles reported by Ketcham and Hobbs [12], giving $\theta_{\mathrm{water\ on\ ice}} = 20°$ (see also refs [11] and [30]). The interpretation of their result [12] in terms of γ_{ice} and $\gamma_{\mathrm{ice\ water}}$ makes less sense, however, as they used Young's equation in what we now know to be an attempt to solve for three unknowns [γ_S^{LW}, $\gamma_S^{\oplus}$, and $\gamma_S^{\ominus}$, which are needed to express $\gamma_S = \gamma_S^{\mathrm{LW}} + 2\sqrt{\gamma_S^{\oplus}\gamma_S^{\ominus}}$; see equations (1) and (4)] with only one equation (i.e. using only one contact angle liquid) (see refs [7] and [8]).

5.5. *The interfacial tension between ice and water*

Utilizing equation (11) and the values given in Table 7, the interfacial tension between ice and water at 0°C can be shown to be close to zero. This is considerably lower than the values compiled by Franks [31] which vary widely between 6.4 and 44 mJ/m^2, using methods such as nucleation, measuring the edge energy of a step on the basal plane of a single crystal, dendrite growth at planes parallel to the *c* axis, morphological stability at planes parallel to the *c* axis, interfacial perturbation, grain boundary groove shapes, and contact angle determination. However, quoting Franks [31]: 'Several comments can be made; first of all, whatever method is chosen for the measurement of γ, theoretical assumptions have to be made as to the effect of surface energy on the process or the measurement. The majority of experimental studies have been based on measurements of homogeneous nucleation; where the results differ, this is largely due to small differences in the equations used to describe nucleation. It has been pointed out that γ obtained from nucleation measurements must not be directly compared with results from macroscopic methods, based on contact angles and grain-groove boundary angles, even if it is permissible to equate the nucleus with ice.' We have already discussed the impossibility of obtaining surface or interfacial tension data by means of contact angle measurements with only one liquid. Contrary to liquid–liquid interfacial tensions between immiscible liquids, which can be readily measured by a variety of methods [32], liquid–solid interfacial tensions cannot be measured directly. Nevertheless, a value of $\gamma_{\text{ice/water}} \approx 0$ remains fairly plausible; for example, on account of the fact that the value of $\gamma_{\text{ice}}^{\text{LW}}$ is somewhat larger than $\gamma_{\text{water}}^{\text{LW}}$, while $\gamma_{\text{ice}}^{\text{AB}}$ is somewhat smaller than $\gamma_{\text{water}}^{\text{AB}}$. On the other hand, the fact that chunks of ice immersed in water at 0°C tend to adhere to each other may argue for a slightly positive value for $\gamma_{\text{ice/water}}$. From the data given in Table 7, using equation (11), $\gamma_{\text{ice/water}}$ at $0°\text{C} = +0.04\ \text{mJ/m}^2$.

6. CONCLUSIONS

(1) From contact angles measured on ice with *cis*-decalin, the Lifshitz–van der Waals component of ice (i) could be determined. Extrapolated to 0°C, this yields $\gamma_i^{\text{LW}} = 29.6\ \text{mJ/m}^2$.

(2) The electron-acceptor ($\gamma_i^{\oplus}$) and electron-donor ($\gamma_i^{\ominus}$) parameters of ice could be derived from contact angle measurements on ice with aqueous solutions of 55% sucrose, and 34% $MgCl_2$, in conjunction with data obtained from the adhesion onto (or exclusion from) advancing freezing fronts of montmorillonite particles and biopolymers. The values thus obtained, extrapolated to 0°C, yield $\gamma_i^{\oplus} = 14$ and $\gamma_i^{\ominus} = 28\ \text{mJ/m}^2$, compared with water at 0°C, for which these values are $26.5\ \text{mJ/m}^2$ for both parameters. Using these two values to obtain the polar (Lewis acid–base) component of the surface tension of ice at 0°C yields $\gamma_i^{\text{AB}} = 39.6\ \text{mJ/m}^2$ [using equation (4)]. The total surface tension of ice is thus $\gamma_i = 69.2\ \text{mJ/m}^2$, which is less than that of water at 0°C: $\gamma_{\text{W}} = 75.8\ \text{mJ/m}^2$. Given, for example, the lower density of ice compared with that of water, this result does not appear to be unreasonable.

(3) From these results, using equation (7), the contact angle of water on ice at 0°C could be calculated to be 24.2°. This is reasonably close to reported experimentally obtained contact angles, which are of the order of 20°.

(4) The interfacial tension between ice and water at 0°C [using equation (1)] is quite small: $\gamma_{i\text{W}} \approx 0.04\ \text{mJ/m}^2$. This value is, however, quite compatible with the known properties of ice–water interactions.

REFERENCES

1. S. N. Omenyi, Ph.D. Thesis, University of Toronto (1978).
2. A. W. Neumann, S. N. Omenyi and C. J. van Oss, *Colloid Polym. Sci.* **257**, 413 (1979).
3. S. N. Omenyi, A. W. Neumann and C. J. van Oss, *J. Appl. Phys.* **52**, 789 (1981).

4. J. K. Spelt, D. R. Absolom, W. Zingg, C. J. van Oss and A. W. Neumann, *Cell Biophys.* **4**, 117 (1982).
5. A. W. Neumann, R. J. Good, C. J. Hope and M. Sejpal, *J. Colloid Interface Sci.* **49**, 291 (1974).
6. T. G. M. van de Ven, P. G. Smith, R. G. Cox and S. G. Mason, *J. Colloid Interface Sci.* **91**, 298 (1983).
7. C. J. van Oss, M. K. Chaudhury and R. J. Good, *Chem. Rev.* **88**, 927 (1988).
8. C. J. van Oss, R. J. Good and M. K. Chaudhury, *Langmuir* **4**, 884 (1988).
9. R. E. Johnson, Jr. and R. H. Dettre, *Langmuir* **5**, 293 (1989).
10. I. D. Morrison, *Langmuir* **5**, 543 (1989).
11. C. A. Knight, *J. Colloid Interface Sci.* **25**, 280 (1967).
12. W. M. Ketcham and P. V. Hobbs, *Philos. Mag.* **19**, 1161 (1969).
13. A. W. Adamson, F. P. Shirley and K. T. Kunichika, *J. Colloid Interface Sci.* **34**, 461 (1970).
14. P. M. Costanzo, R. F. Giese and C. J. van Oss, *J. Adhesion Sci. Technol.* **4**, 267 (1990).
15. J. J. Jasper, *J. Phys. Chem. Ref. Data* **1**, 841 (1972).
16. C. J. van Oss, R. F. Giese and P. M. Costanzo, *Clays Clay Minerals* **38**, 151 (1990).
17. C. J. van Oss, M. K. Chaudhury and R. J. Good, *Adv. Colloid Interface Sci.* **28**, 35 (1987).
18. C. J. van Oss, *J. Protein Chem.* **8**, 661 (1989).
19. C. J. van Oss, *J. Protein Chem.* **9**, 487 (1990).
20. L. A. Haff, *Prep. Biochem.* **9**, 149 (1979).
21. A. Castro and A. Ehrlich, *Transfusion* **6**, 594 (1966).
22. C. J. van Oss, *Cell Biophys.* **14**, 1 (1989).
23. C. J. van Oss, in: *Biophysics of the Cell Surface*, R. Glaser and D. Gingell (Eds), p. 131. Springer Verlag, Berlin (1990).
24. R. F. Giese, C. J. van Oss, J. Norris and P. M. Costanzo, *Proc. 9th Int. Clay Conf.*, Strasbourg, pp. 33–41 (1989).
25. J. Kloubek, *J. Colloid Interface Sci.* **46**, 185 (1974).
26. M. K. Chaudhury, Ph.D. Thesis, SUNY at Buffalo (1984).
27. V. LeFebre, *J. Colloid Interface Sci.* **25**, 263 (1967).
28. G. W. Gross, *J. Colloid Interface Sci.* **25**, 270 (1967).
29. R. E. Allen, P. H. Rhodes, R. S. Snyder, G. H. Barlow, M. Bier, P. E. Bigazzi, C. J. van Oss, R. J. Knox, G. V. F. Seaman, F. J. Micale and J. W. Vanderhoff, *Separ. Purif. Methods* **6**, 1 (1977).
30. C. A. Knight, *Proc. Int. Conf. Cloud Phys.*, Toronto, p. 204 (1968).
31. F. Franks (Ed.), in: *Water*, vol. 7, p. 215. Plenum Press, New York (1982).
32. A. W. Adamson, *Physical Chemistry of Surfaces*, p. 27. Wiley-Interscience, New York (1982).